Derivation of the Analytical Solution of the Thermal Conduction-Convection Equation under Fourier Series Boundary Conditions

Y. Li[1,2], X. Gao[1,2*], L. Yang[1,2], Z. Li[1,2], Y. Zhou[3]

[1]Key Laboratory of Land Surface Process and Climate Change in Cold and Arid Regions of Chinese Academy of Sciences, Northwest Institute of Eco-Environment and Resources, Chinese Academy of Sciences, 320, Donggang West Road, Lanzhou, Gansu, 730000, China.

[2]University of Chinese Academy of Sciences, Beijing 100049, China.

[3]Qufu Normal University, 80, Yantai Road, Donggang District, Rizhao, Shandong, 276826, China.

Corresponding author：

X. Gao, xqgao@lzb.ac.cn

Key points:

• The precision of amplitude method, phase method, logarithmic method, arctangent method is not high enough.

• When the soil temperature is simulated by the Fourier series, as the order n becomes larger, the result becomes more accurate.

Abstract

The thermal properties of soil play important roles in biogeochemical cycles. The soil thermal diffusivity can accurately reflect the transient process of soil heat conduction. In this study, we use observation data from the 5, 10, 20, 40, and 80 cm layers in Golmud from October 2012 to July 2013 and comprehensively compare the solution of soil thermal diffusivity thereafter. A new model is established using the thermal conduction-convection equation under Fourier boundary conditions. The results show that (1) the amplitude method and the phase method are based on a single temperature sine wave, which is used to describe the general soil, although the accuracy is not high enough; the logarithmic method and the arctangent method are performed four times a day, the accuracy of the obtained result is also low; moreover, the Laplace method does not have a clear soil temperature boundary function and thus can better address extreme weather effects or nonperiodic changes in soil temperature. (2) When solving the thermal conduction equation by a numerical method, format 2 (Crank-Nichalson-Sch format) is unconditionally stable, the data utilization is higher; in addition, the obtained soil thermal diffusivity is less discrete, and the result is more accurate. (3) When the soil temperature is simulated by the Fourier series, as the order n becomes larger, the result becomes more accurate. The Fourier series performs well in simulating the soil thermal properties. This study provides a useful tool for calculating soil thermal diffusivity, which may help to further characterize biogeochemical cycles.

Plain language summary

Soil is an extremely important part of biogeochemical cycling. Soil enzymes have been used as indicators of biogeochemical cycles, organic matter degradation, and soil remediation processes. Changes in soil thermal properties change the soil enzyme activity, plant productivity and nitrogen uptake as well as the living conditions of soil microorganisms .Therefore, studying the thermal properties of soil is of great significance for understanding the biogeochemical cycle. We used the soil temperature data of the Golmud photovoltaic power station and used a variety of methods to calculate the soil thermal diffusivity at different levels. We found that using Fourier series to calculate the soil thermal diffusivity and simulate soil temperature is more accurate.

1 Introduction

Soil is an extremely important part of biogeochemical cycling (Oelke & Zhang, 2004). Soil enzymes reveal ecosystem perturbations and have been used as indicators of biogeochemical cycles, organic matter degradation, and soil remediation processes (Lee et al., 2020). The thermal properties of the soil are a key variable in the growth and decomposition of above- and belowground biomass (Abramoff & Finzi, 2015; Munir et al., 2015; Wang et al., 2013; Xu et al., 2013). Changes in soil thermal properties change the soil enzyme activity, plant productivity and nitrogen uptake as well as the living conditions of soil microorganisms (Luo et al., 2009; Rustad et al., 2001). Studying soil thermal properties is of great significance for understanding biogeochemical cycling (Hillel, 2014; Usowicz, 1996). Temperature is an important physical variable of soil and plays a critical role in energy balance applications, including land surface modeling, climate prediction and numerical weather forecasting (Zhang et al., 2011). Previous works have shown that the soil temperature response to atmospheric climate change can be complex (Fang et al., 2010). Soil temperature affects the physical and chemical properties of the soil as well as other biochemical processes, further affecting the biochemical processes of plant growth (Zhang et al., 2012). The heat transfer in the soil is mainly carried out by heat conduction and convection. The speed of soil temperature wave propagation is expressed by the thermal diffusivity (Zhang et al., 2011). Soil thermal conductivity, thermal diffusivity and soil heat capacity are three significant soil thermal properties (Yue et al., 2011). Soil thermal conductivity and thermal diffusivity are related to soil heat capacity; therefore, only one of them needs to be determined. The usual choice is the soil thermal diffusivity, which reflects the transient process of heat transfer. Understanding the soil thermal diffusivity can not only further grasp the thermodynamic properties of soil but also provide the necessary conditions for the simulation of heat flux and soil temperature (Liu et al., 2012).

Shallow surface heat transfer is the heat transfer of soil or rock at a depth of ten meters below the surface. The shallow surface medium is connected to the atmosphere and the earth's crust. Research on heat transfer plays an important role in understanding the atmosphere, the interior of the earth and the coupling between the two (Bhumralkar, 1975; Dai et al., 2009; Li et al., 2015; Zheng & Liu, 2013). Accurately simulating the temperature, heat flux and soil thermal diffusivity of shallow surface soils is an important part of the numerical simulation of land surface processes, atmospheric circulation and regional climate. Therefore, many researchers have carried out a large number of experiments on soil thermodynamic properties and parameterization of land surface processes (Horton et al., 1983; Liu et al., 2014; Shao et al., 1998).

The thermal diffusivity can be determined based on the observed soil temperature in a variety of ways, most of which are based on the assumption that soil is a semiunbounded medium with a constant thermal diffusivity and that the upper thermal boundary can be expressed by a harmonic function (Li et al., 2015; Zheng & Liu, 2013). In terms of the thermal conduction equation for soil temperature (SCM), the common calculation methods include the amplitude method, phase method, arctangent method, logarithmic method, numerical method, harmonic method, Laplace method, and modified Laplace method. Several of these methods have been evaluated under the assumption that the temperature at the upper boundary can be well described by a sinusoidal function or by a Fourier series. Studies have shown that the Fourier series is relatively reliable. For the nonperiodic soil temperature, the Laplace method and the modified Laplace method are closer to the real soil heat conduction process, although the calculation of the two has some complexity (Liu et al., 2014).

Under many soil conditions, vertical water vapor flux affects soil temperature, and the thermal conduction-convection equation for soil temperature (SCCM) helps to address such conditions. Studies have shown that the soil temperature determined by the thermal conduction-convection equation for soil temperature is more favorable than the measured multilayer depth soil temperature (Horton et al., 1983). Other studies have shown that changes in soil temperature are related to soil thermal conductivity and soil thermal convection caused by vertical liquid motion (Goto et al., 2005; Kane et al., 2001). Therefore, the thermal conduction-convection equation for soil temperature (SCCM) has a higher ability to describe the soil heat transfer process than the thermal conduction equation (SCM).

Since the 20th century, scholars have proposed many methods for calculating the thermal diffusivity of soil. Whether based on SCMs, SCCMs, or different soil thermodynamic properties, these methods have their own applicable conditions, advantages and disadvantages. Previous work led to important contributions, although the horizontal comparison of various methods was relatively insufficient. Therefore, the objectives of the present study were to (1) transversely compare the results of soil thermal diffusivity obtained from different boundary conditions under the SCM; (2) derive a method of solving the SCCM under the condition of a Fourier boundary and obtain the thermal diffusivity; and (3) compare the measured soil temperature with the soil temperature obtained by solving the SCCM under the Fourier boundary condition.

2 Field experiments

Golmud ($91°25'$ $95°12'$,$35°10'$ $37°45'$) is located in the western part of Qinghai Province, the hinterland of the Qinghai-Tibet Plateau. This area is composed of two unconnected parts: the central and southern parts of the Qaidam Basin and Tanggula Mountain. The average temperature in Golmud is 5.3 °C, the precipitation is 42.1 mm, the relative humidity is 32%, the cumulative number of sunshine events is 3096.3 h, and the accumulated annual evaporation is 2504.1 mm. It belongs to the continental plateau climate and presents less rain, wind and drought. The annual average sunshine hours in the region are 3200~3600 h, and the annual total solar radiation is 6618~7356 MJ/m^2. It is the second largest high-value solar radiation area in China after the Qinghai-Tibet Plateau (Yang et al., 2017).

The observation station ($36°20.128' N, 95°13.372' E$) used in this study is located inside the photovoltaic power station, with an altitude of approximately 2927 m. The soil temperature used in this study was recorded every 10 minutes by CR1000 produced by Campbell Corporation of the United States at 6 depth layers of 5 cm, 10 cm, 20 cm, 40 cm, 80 cm, and 180 cm for the period from October 2012 to July 2013. The data were quality controlled (Gao et al., 2016).

3 Method

3.1 Thermal conduction equation for soil temperature (SCM)

The volumetric heat capacity $C_g (J \cdot cm^{-3} \cdot K^{-1})$ and the soil thermal conductivity λ ($W \cdot m^{-1} \cdot K^{-1}$) are assumed to remain consistent with depth based on the classical thermal diffusion equation in a one-dimensional semiunbounded medium:

$$\frac{\partial T}{\partial T} = k \frac{\partial^2 T}{\partial z^2} (1)$$

where $k = \lambda / C_g$ (unit: $m^2 s$) is the thermal diffusivity.

The boundary condition at z_1 is given by the following equation (Van Wijk & de Vries, 1963):

$$T ¿_{z=z1} = \overline{T_1} + A_1 \sin(\omega t - \Phi_1), t \geq 0 (2)$$

where $\overline{T_1}$ (°C) is the average value of soil temperature at depth z_1, A_1 (°C) is the amplitude, ω=2π/p (rad/s) is the daily change period, p is the period of the change, and Φ_1 is the initial soil temperature (primary phase) (rad) at depth z_1, which is obtained by least squares fitting.

According to Eq. (1) and Eq. (2), the soil temperature at depth z_2 is expressed as follows:

$$T_{z=z2} = \overline{T_2} + A_1 \exp[(z_1 - z_2)\alpha] \sin[\omega t - \Phi_1 - (z_2 - z_1)\alpha] (3)$$

where $\alpha = \sqrt{\omega / 2k}$. The amplitude A_2 and initial phase Φ_2 at depth z_2 are as follows:

$$A_2 = A_1 \exp[-(z_2 - z_1)\alpha]$$

$$\Phi_2 = \Phi_1 + (z_2 - z_1)\alpha$$

According to Eq. (1) to Eq. (3), the thermal diffusivity k can be expressed with the amplitude and phase:

$$k_P = \text{¿}$$

$$k_A = \text{¿}$$

3.1.1 Arctangent method and logarithmic method

Soil temperatures can be simulated with a series of sinusoidal terms. Observations of soil temperature at a certain depth can be expressed in Fourier series:

$$T(t)=\overline{T}\cdot\sum_{n=1}^{2}[A_n\cos(n\omega t)+B_n\sin(n\omega t)](6)$$

where $\overline{T}$ (°C) is the average value of soil temperature and A_n and B_n (°C) are amplitudes. Eight soil temperature observations were performed at two depths per day. The phase method is shown in Eq. (4):

$$k=\omega\text{¿}$$

¿

where $T_1(z_1)$, $T_2(z_1)$, $T_3(z_1)$, $T_4(z_1)$ and $T_1(z_2)$, $T_2(z_2)$, $T_3(z_2)$, $T_4(z_2)$ are four soil temperature observations at z_1 and z_2.

The amplitude method is shown in Eq. (5):

$$k=\frac{\omega}{2}\times\frac{z_2-z_1}{\{\ln\text{¿¿¿}}$$

Eq. (7) is an arctangent method, and Eq. (8) is a logarithmic method, which was developed early without automatic recording equipment. Compared with the phase method in Eq. (4) and amplitude method in Eq. (5), the arctangent method and the logarithmic method do not need to fit the amplitude and phase; thus, they are simpler and more convenient to use and have the ability to reflect the possible nonsinusoidal changes (Liu et al., 1991). However, the temperature sampling data at intervals of 6 h will inevitably lead to the absence of short-period signals. When the heat transfer model is established, there are no high-order harmonic components with boundary conditions, which leads to further errors in the simulation results (Liu et al., 2014).

3.1.2 Laplace transformation based method (LTM)

In Section (3.1.1), the prerequisite for the four methods is to assume a stable cyclical change in soil temperature. In actual circumstances, if there is a sudden change in weather conditions, such as heavy precipitation, cold waves, blizzards, etc., then the stability cycle will fail. Therefore, the model with stable period change as the boundary condition will not be applicable when simulating soil temperature change and obtaining thermal diffusivity (Liu et al., 2014). To better simulate the nonperiodic changes in soil temperature and make the boundary conditions of the model closer to the soil heat transfer process, the Laplace transform is a good choice.

The solution of Eq. (1) with initial and boundary conditions is given as follows:

$$T(z,0)=T_0 \quad (9a)$$

$$T(0,t)=\Phi(t),\, t>0 \quad (9b)$$

Then, the Laplace transformation can be performed (Carslaw & Jaeger, 1959):

$$T(z,t)=T_0+\frac{z}{2\sqrt{\pi k}}\int_0^t \Phi(\tau)\frac{\exp\left(\frac{-z^2}{4k(t-\tau)}\right)}{(t-\tau)^{3/2}}d\tau \quad (10)$$

Eq. (10) applies to a semi-infinite medium whose upper boundary condition is given by Φ(t), a continuous function of time. It is an impulse response equation that is useful for sudden changes in temperature input signals (such as in rainy or cold front transit). A limitation of using this equation is that the initial temperature profile must be uniform. The soil thermal diffusivity can be obtained by fitting Eq. (10) (de Silans et al., 1996).

3.1.3 Numerical method

For homogeneous soils, the heat transfer equation can be approximated by a difference equation. Commonly used differential formats are as follows (Liu et al., 1991):

(1) Dufeat-Frankel-Sch (format 1)

$$\frac{T_j^{n+1}-T_j^n}{2}=\frac{k\,\Delta t}{\Delta z^2}\left(T_{j+1}^n+T_{j-1}^n-T_j^{n+1}-T_j^{n-1}\right) \quad (11)$$

This format is stable.

(2) Crank-Nichalson-Sch (format 2)

$$T_j^{n+1}-T_j^n=\frac{k\Delta t}{2\Delta z^2}\left[\left(T_{j+1}^{n+1}-2T_j^{n+1}+T_{j-1}^{n+1}\right)+\left(T_{j+1}^n-2T_j^n+T_{j-1}^n\right)\right](12)$$

This format is unconditionally stable. In Eq. (11)-(12), j represents a spatial interval and n represents a time interval.

3.2 Thermal conduction-convection equation for soil temperature (SCCM)

Eq. (1) assumes that the soil is vertically uniform. However, some scholars (Gao et al., 2003) believe that the difference between day and night temperature and solar radiation will trigger the vertical movement of soil water, which affects the temperature distribution in soil. To reflect the influence of this part, heat conduction was combined with convection to establish a soil heat conduction-convection model:

$$\frac{\partial T}{\partial t}=k\frac{\partial^2 T}{\partial z^2}-\frac{C_W}{C_g}w\theta\frac{\partial T}{\partial z}(13)$$

where w (m/s) is the liquid flow rate (downward positive), θ is the volumetric water content of the soil, and C_W ($J\,℃^{-1}m^{-3}$) is the specific heat capacity of the water. Assume that these quantities are independent of z and $\frac{-C_W}{C_g}w\theta$ is the liquid water flux density. Let

$W=\frac{-C_W}{C_g}w\theta\frac{\partial T}{\partial z}$, then:

$$\frac{\partial T}{\partial t}=k\frac{\partial^2 T}{\partial z^2}+W\frac{\partial T}{\partial z}(14)$$

3.2.1 Boundary condition as a superposition of a sine wave on the constant temperature field

Given the following boundary condition:

$$T|_{z=0}=\overline{T}+A\sin\omega t\,(t\geq 0)$$

The solution of Eq. (14) is as follows:

$$T(z,t)=T_0+A\exp\left[\left(\frac{-W-\alpha}{2k}\right)z\right]\sin\left(\omega t-\Phi_1-\frac{\beta}{2k}z\right)(15)$$

where

$$\alpha=\sqrt{\frac{W^2+\sqrt{W^4+16k^2\omega^2}}{2}}\;,\quad \beta=\frac{2\sqrt{2}k\omega}{\sqrt{W^2+\sqrt{W^4+16k^2\omega^2}}}(16)$$

Therefore, the soil temperature (T) at depth z_2 can be calculated using the following equation:

$$T_{z=z2}=\overline{T}_2+A_1\exp\left[\left(z_1-z_2\right)\alpha M\right]\sin\left[\omega t-\Phi_1-\left(z_2-z_1\right)\alpha N\right](17)$$

In Eq. (17), M and N can be expressed as follows:

$$M=\frac{\alpha}{\omega}\{W+\frac{1}{\sqrt{2}}\text{¿}$$

$$N=\sqrt{2}\frac{\omega}{\alpha}\text{¿}$$

Assuming that $z_1<z_2,A_1>A_2,\Phi_1<\Phi_2$, the following equations are derived (Gao, 2005):

$$k=-\text{¿¿}$$

$$W=\frac{\omega\left(z_2-z_1\right)}{\Phi_2-\Phi_1}\text{¿}$$

The above is the thermal conduction-convection method.

3.2.2 Boundary condition as the form of Fourier series

Hu et al. (2015) derived the thermal conduction-convection equation for the Fourier series boundary of soil temperature (FFCM). Given the following boundary condition:

$$T\left(0,t\right)=T_0+\sum_{n=1}^{N}A_n\sin\left(n\omega t-\Phi_n\right),n=1,2,\ldots,N\left(20\right)$$

where n is the number of harmonics.

The solution of Eq. (15) is as follows:

$$T\left(z,t\right)=T_0+\sum_{n=1}^{N}A_n\times\exp\left[\left(\frac{-W}{2k}-\frac{\sqrt{2}}{4k}X_n\right)z\right]\sin\left(n\omega t-\frac{\sqrt{2}\omega}{nX_n}z\right)(21)$$

where

$$\alpha_n=\sqrt{\frac{{W_n}^2+\sqrt{{W_n}^4+16{k_n}^2\omega^2}}{2}}\;,\quad \beta_n=\frac{2\sqrt{2}k_n\omega}{\sqrt{{W_n}^2+\sqrt{{W_n}^4+16{k_n}^2\omega^2}}}$$

Therefore, the soil temperature (T) at depth z_2 can be calculated using the following equation:

$$T_{z=z2}=\overline{T}_2+\sum_{n=1}^{N} A_n \exp\left[\left(\frac{-W-\alpha_n}{2k}\right)(z_2-z_1)\right]\times \sin\left[n\omega t-\Phi_n-(z_2-z_1)\frac{\beta_n}{2k}\right] (22)$$

3.2.3 Derivation of k_n under Fourier series boundary condition

According to the derivation of the conduction convection method by Gao (2005), we can derive the solution of the soil thermal diffusivity under Fourier series boundary conditions.

A_n^1, Φ_n^1 and A_n^2, Φ_n^2 under the Fourier series boundary condition can be expressed as follows:

$$A_n^1=A_n\times z_1 e^{\left(\frac{-W}{2k}-\frac{\sqrt{2}}{4k}X_n\right)} (23a)$$

$$\Phi_n^1=\frac{\sqrt{2}\,\omega z_1}{n X_n} (23b)$$

$$A_n^2=A_n\times z_2 e^{\left(\frac{-W}{2k}-\frac{\sqrt{2}}{4k}X_n\right)} (23c)$$

$$\Phi_n^2=\frac{\sqrt{2}\,\omega z_2}{n X_n} (23d)$$

where A_n^1, Φ_n^1 and A_n^2, Φ_n^2 are the amplitude and phase of the nth term of the Fourier series at depths z_1 and z_2, respectively; and $X_n=\sqrt{W_n{}^2+\sqrt{W_n{}^4+16k_n{}^2\omega^2}}$.

Assuming that $z_1>z_2$ (that is, $A_n^1<A_n^2$, $\Phi_n^1>\Phi_n^2$), the following is obtained:

$$\frac{\ln\left(A_n^1/A_n^2\right)}{z_1-z_2}=\left(\frac{-W}{2k}-\frac{\sqrt{2}}{4k}X_n\right) (24)$$

From Eq. (23b) and Eq. (23d), the following can be concluded:

$$X_n=\frac{\sqrt{2}\,\omega(z_1-z_2)}{n\left(\Phi_n^1-\Phi_n^2\right)} (25)$$

Combining Eq. (24) with Eq. (25), the following is obtained:

$$k_n^2=\frac{(z_1-z_2)^2\cdot\left[W_n+\omega\cdot\frac{z_1-z_2}{n\left(\Phi_n^1-\Phi_n^2\right)}\right]^2}{4\ln^2\left(A_n^1/A_n^2\right)}=\frac{(z_1-z_2)^2\cdot\left[nW_n\left(\Phi_n^1-\Phi_n^2\right)+\omega(z_1-z_2)^2\right]}{4n^2\left(\Phi_n^1-\Phi_n^2\right)^2\ln^2\left(A_n^1/A_n^2\right)} (26)$$

Eq. (26) can be rewritten as follows:

$$k_n^2 = \frac{(z_1 - z_2)^2}{4n^2(\Phi_n^1 - \Phi_n^2)^2}\left[\frac{\omega^2(z_1 - z_2)^2}{n^2(\Phi_n^1 - \Phi_n^2)^2} - W^2\right] \quad (27)$$

Eq. (26) and Eq. (27) are combined to eliminate k_n and obtain an equation for W_n:

$$\left[nW_n(\Phi_n^1 - \Phi_n^2) + \omega(z_1 - z_2)\right]^2 = \ln^2\left(\frac{A_n^1}{A_n^2}\right)\left[\frac{\omega^2(z_1 - z_2)^2}{n^2(\Phi_n^1 - \Phi_n^2)^2} - W_n^2\right] \quad (28)$$

Eq. (28) can be rewritten as follows:

$$aW_n^2 + bW_n + c = 0 \quad (29)$$

where

$$\begin{cases} a = n^4(\Phi_n^1 - \Phi_n^2)^4 + n^2(\Phi_n^1 - \Phi_n^2)^2 \cdot \ln^2(A_n^1 / A_n^2) \\ b = 2n^3\omega(\Phi_n^1 - \Phi_n^2)^3(z_1 - z_2) \\ c = \omega^2(z_1 - z_2)\left[n^2(\Phi_n^1 - \Phi_n^2)^2 - \ln^2(A_n^1 / A_n^2)\right] \end{cases} \quad (30)$$

According to Eq. (29), the value of W_n is not always negative:

$$W_n = \frac{\omega(z_1 - z_2)}{n(\Phi_n^1 - \Phi_n^2)}\left[\frac{2\ln^2\left(\frac{A_n^1}{A_n^2}\right)}{n^2(\Phi_n^1 - \Phi_n^2)^2 + \ln^2\left(\frac{A_n^1}{A_n^2}\right)} - 1\right] \quad (31)$$

$$k_n = \frac{-(z_1 - z_2)^2\,\omega\ln\left(\frac{A_n^1}{A_n^2}\right)}{n(\Phi_n^1 - \Phi_n^2)\left[n^2(\Phi_n^1 - \Phi_n^2)^2 + \ln^2\left(\frac{A_n^1}{A_n^2}\right)\right]} \quad (32)$$

4 Result

4.1 Comparison of five methods for the thermal conduction equation in the shallow soil layer

The soil thermal diffusivities at six depths (5-10 cm, 5-20 cm, 5-40 cm, 10-20 cm, 10-40 cm, and 20-40 cm) in the shallow soil of the photovoltaic power station were calculated by the amplitude method, phase method, arctangent method, logarithm method and Laplace method.

The boundary condition of the amplitude method and the phase method is that a constant sine wave is superimposed on the constant temperature field. Selecting the parts of the fitting result whose judgment coefficients are greater than 0.8 (Wang et al., 2019), Figure 1c, e and f show that there are fewer data with coefficients of determination greater than 0.8 at 40 cm and the fitting result is not good. Figure 1 shows that the results obtained by the amplitude method at the four levels of 5-10 cm, 5-20 cm, 5-40 cm, and 10-20 cm are generally larger than that of the phase method. Compared with the amplitude method, the phase method can partially reflect the extreme values of the thermal diffusivity. Figure 2 shows that the arctangent method is derived from the phase method. In addition, 0, 8, 16 and 24 (Beijing time) points are selected every day and the obtained soil thermal diffusivity results are more uniform. Compared with the phase method, it does not reflect some extreme conditions. The logarithm method is derived from the formula of the amplitude method. The time of selection was based on 0, 8, 16 and 24 (Beijing time) points. The results obtained by the logarithm method are similar to those obtained by the amplitude method. However, some extreme values reflected by the amplitude method are not reflected in the logarithmic method. At depths of 5-40 cm, the soil thermal diffusivity obtained by the amplitude method, the phase method, the arctangent method and the logarithm method have large differences. The Laplace method does not have a formula for the established boundary conditions. Figure 3 shows that the method is effective in reflecting the influence of some extreme conditions and nonperiodic weather changes on the thermal diffusivity. The above results are basically consistent with the results obtained by Liu et al. (1991). The amplitude method and phase method are based on a single temperature sine wave, which is used to describe the general soil, and the accuracy is not high enough, especially when there are multiple extreme temperature values. The arctangent method and logarithmic method require less measured data and present more convenient data acquisition, which is one of the main reasons for their lack of precision, and they also inherit some of the disadvantages of the amplitude method and phase method. The Laplace method has no fixed boundary condition function, and it has outstanding advantages in dealing with actual weather conditions, such as sudden weather, heavy precipitation, cold waves, blizzards and other nonperiodic weather changes.

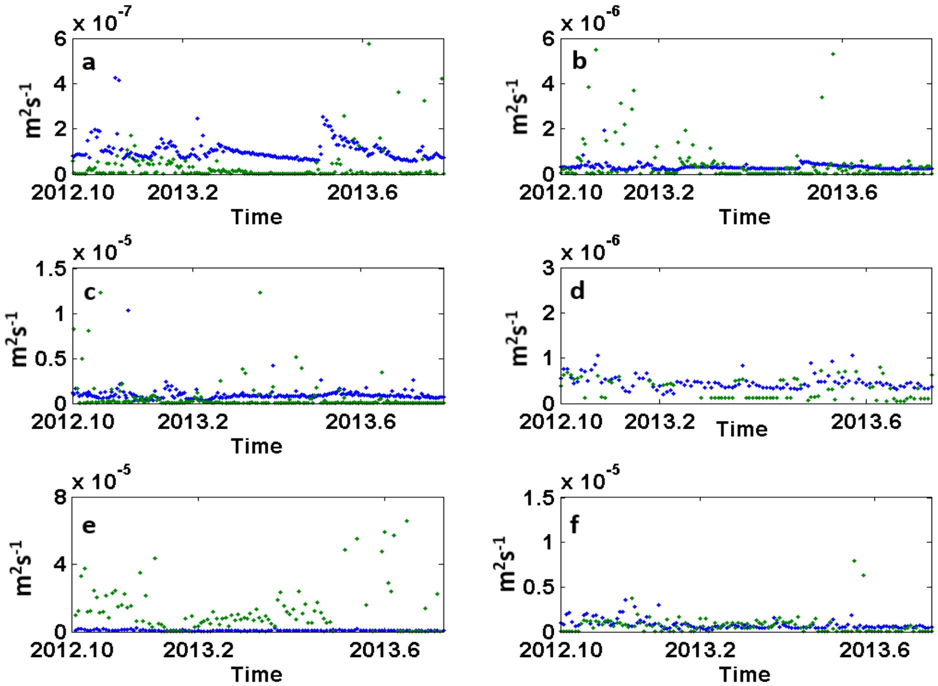

Figure 1. Soil thermal diffusivities at six different depths calculated by the amplitude method and phase method. **a**. 5-10 cm, **b**. 5-20 cm, **c**. 5-40 cm, **d**. 10-20 cm, **e**. 10-40 cm, and **f**. 20-40 cm. Blue represents the amplitude method, and green represents the phase method.

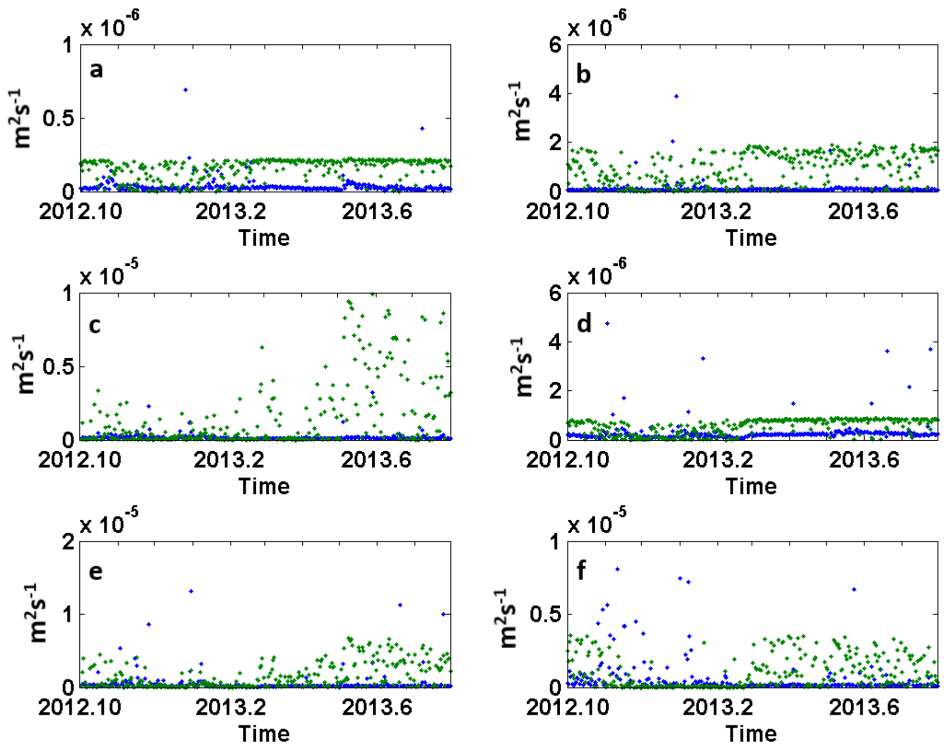

Figure 2. Soil thermal diffusivities at six different depths calculated by the logarithmic method and arctangent method. **a**. 5-10 cm, **b**. 5-20 cm, **c**. 5-40 cm, **d**. 10-20 cm, **e**. 10-40 cm, and **f**. 20-40 cm. Blue stands for arctangent, and green stands for logarithm

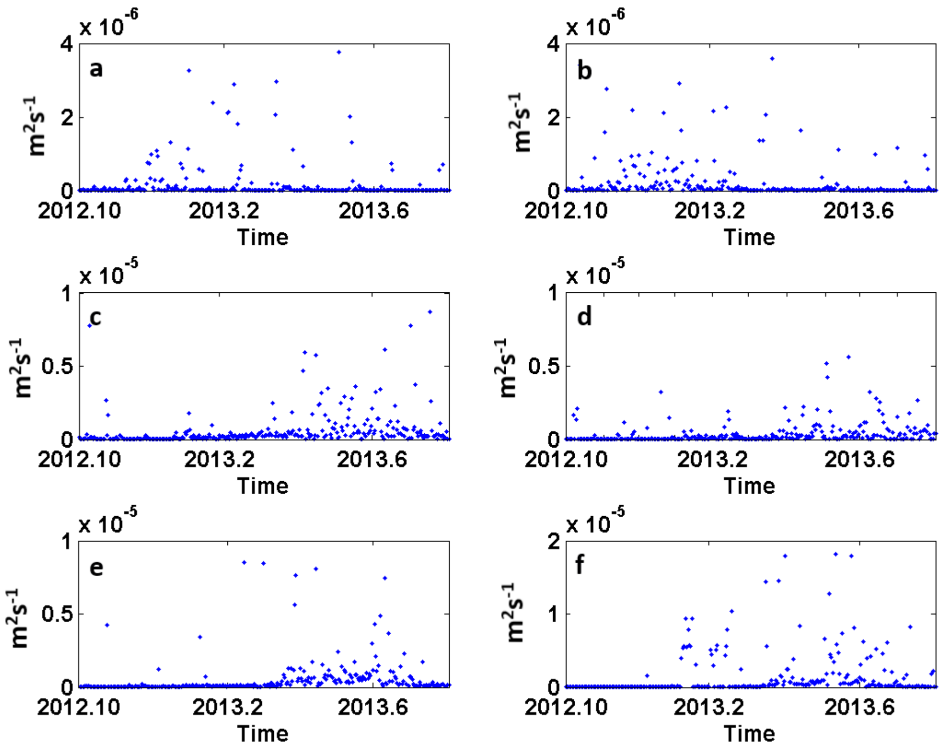

Figure 3. Soil thermal diffusivities at six different depths calculated by the Laplace method. **a**. 5-10 cm, **b**. 5-20 cm, **c**. 5-40 cm, **d**. 10-20 cm, **e**. 10-40 cm, and **f**. 20-40 cm.

4.2 Analysis of numerical methods for the thermal conduction equation

Two differential formats are used, namely, format 1 (Dufeat-Frankel-Sch) and format 2 (Crank- Nichalson-Sch), and the heat transfer equation is solved in 10-minute steps. The results are shown in Figure 4. The three different depths (5-20 cm, 5-40 cm, 10-40 cm) of soil thermal diffusivity obtained by the two methods in Figure 4 have two peaks between December 2012 and June 2013. The thermal diffusivity changes obtained in the two formats are generally the same, but the dispersion of k values in the second format is small. Between the two, although format 1 is stable, the data utilization is less than that of format 2 and the precision is lower. The second format is unconditionally stable, and the data utilization rate is high; therefore, the degree of dispersion is small, and the precision is higher. Liu et al. (1991) pointed out that on a sunny day with few clouds, the numerical method needs to measure 12 data points from 3 depths; and when the weather is cloudy, it is necessary to measure 24 data points from 3 depths with high precision. In the case of a shortened time interval, the relative bias will also decrease; in both formats, format 2 has higher precision and neither of them needs to reduce Δz or Δt to ensure stability.

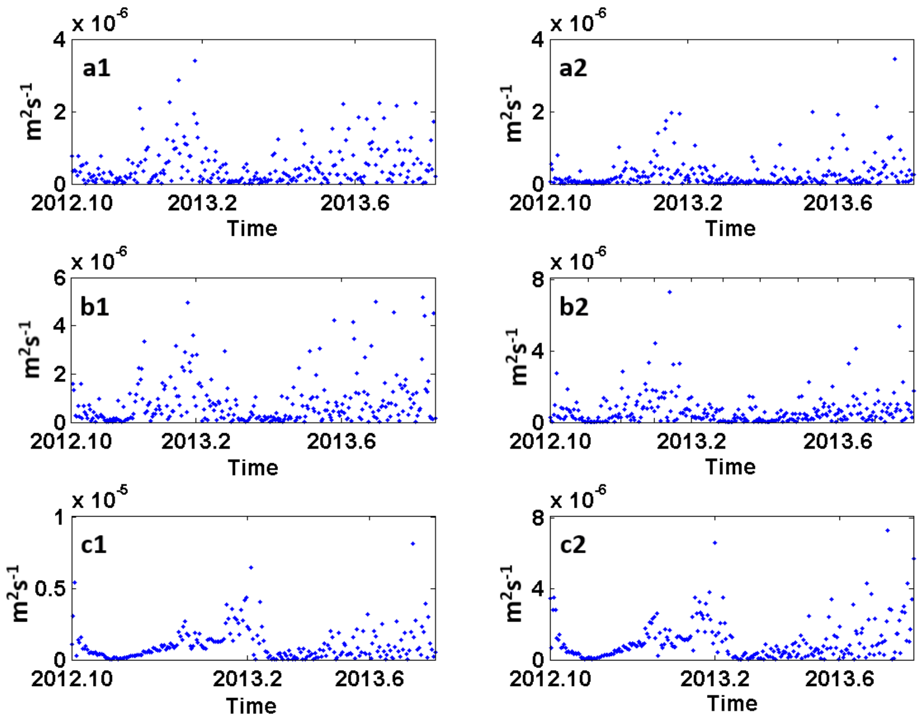

Figure 4. Soil thermal diffusivities at three different depths calculated by format 1 (Dufeat-Frankel-Sch) and format 2 (Crank-Nichalson-Sch). **a**1, **a**2. 5-20 cm; **b**1, **b**2. 5-40 cm; and **c**1, **c**2. 10-40 cm.

4.3 Analysis of the results of the thermal conduction-convection equation under Fourier series boundary conditions

4.3.1 First-order Fourier series (thermal conduction-convection)

In Figure 5, the thermal conduction-convection method is a special case (first-order) of the thermal conduction-convection equation under the Fourier boundary condition. Traditional algorithms assume that the soil is vertically uniform and only consider heat transfer; the thermal conduction-convection equation considers the vertical heterogeneity in the soil and combines the effects of upward heat convection (water transport) on soil temperature. Comparing the results of the thermal conduction-convection method with the previous methods, the thermal conduction-convection method is more sensitive to the change in soil thermal diffusivity and can better reflect the change in soil thermal diffusivity with weather. The main disadvantage of the traditional thermal conduction equation is that when the vertical gradient of soil thermal diffusivity is relatively large, it overestimates the amplitude and phase of the soil temperature; therefore, it is only suitable for estimating the actual soil temperature of vertically uniform dry soil (Gao, 2005).

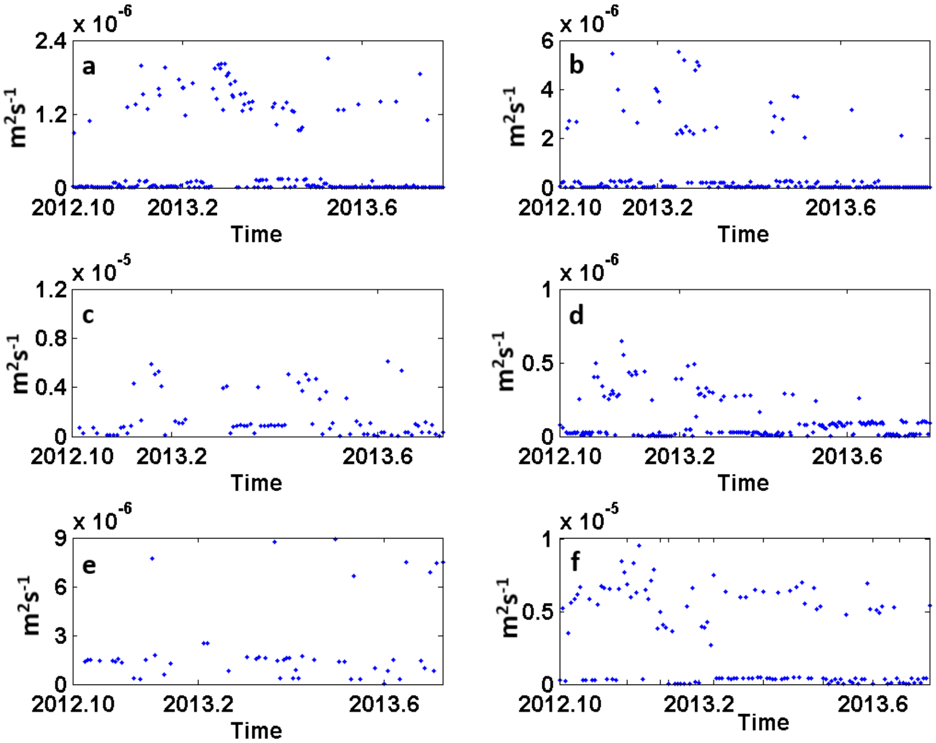

Figure 5. Soil thermal diffusivities of six different depths on the surface calculated by the first-order Fourier series (thermal conduction-convection method). **a**. 5-10 cm, **b**. 5-20 cm, **c**. 5-40 cm, **d**. 10-20 cm, **e**. 10-40 cm, and **f**. 20-40 cm.

4.3.2 Second-order, third-order and fourth-order Fourier series

In Figure 6, Figure 7 and Figure 8, the Fourier series, which is a special case of the Fourier integral, is one of the classical methods for analyzing the continuity of periodic signals. When performing Fourier series decomposition on a computer, the continuous signal is sampled and then decomposed according to the discrete Fourier series. Any periodic continuous signal can be decomposed into a set of rotation vectors according to the Fourier series (Ahmed & Rao, 1975; Liang, 1982). The soil thermal diffusivity is difficult to change, and it has a certain periodicity most of the time; therefore, it is reasonable to use the Fourier series. Fourier decomposition is essentially a filtering process (Duan et al., 2016). The fitted nth-order phase Φ_n

and the amplitude A_n are substituted into Eq. (32) to obtain the value of k_n, which is the contribution of different wave components to the soil thermal diffusivity k. These soil thermal diffusivity components k_n can be superimposed to obtain a more accurate change in the soil thermal diffusivity k. As the order n becomes larger, the simulated soil thermal diffusivity k will be more accurate.

Second-order:

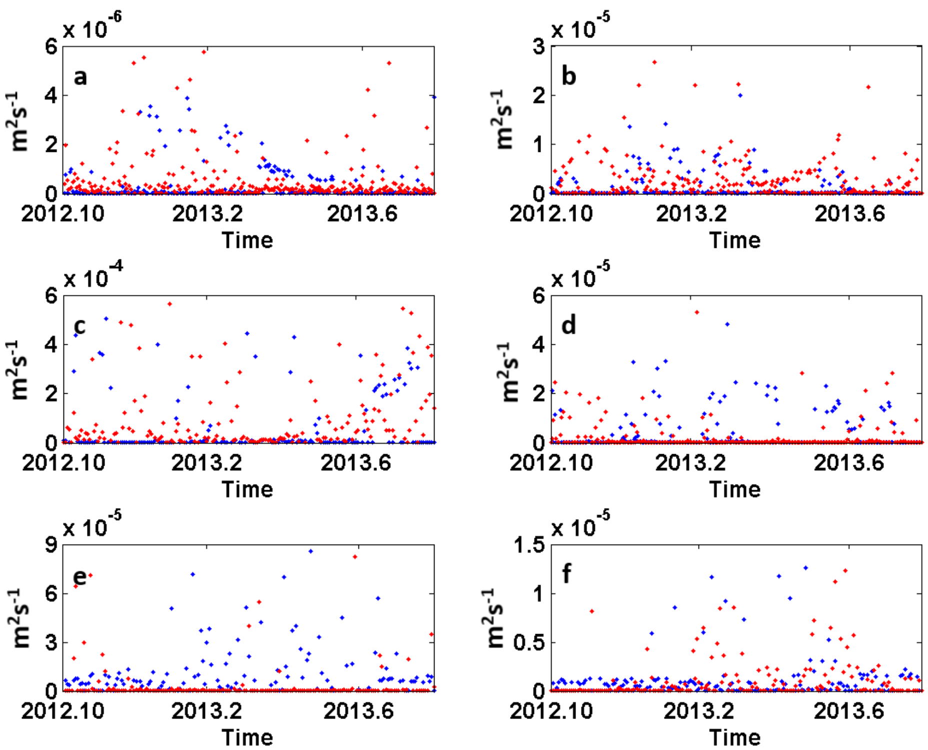

Figure 6. Soil thermal diffusivities of six different depths on the surface calculated by second-order Fourier series. **a**. 5-10 cm, **b**. 5-20 cm, **c**. 5-40 cm, **d**. 10-20 cm, **e**. 10-40 cm, and **f**. 20-40 cm. Blue for k1, and red for k2.

Third-order:

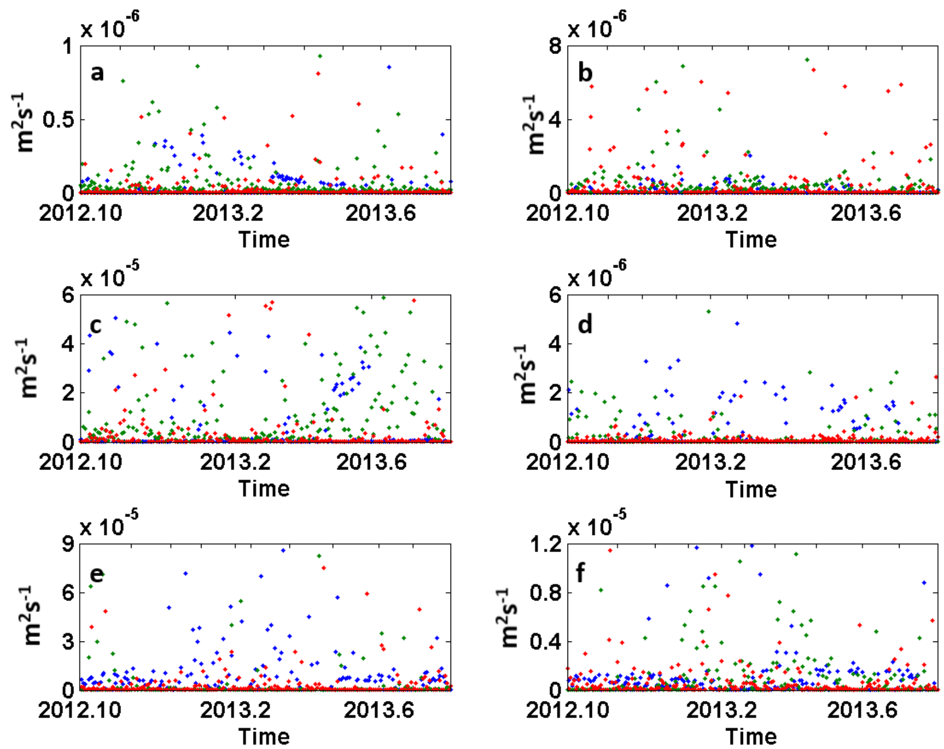

Figure 7. Soil thermal diffusivities of six different depths on the surface calculated by third-order Fourier series. **a**. 5-10 cm, **b**. 5-20 cm, **c**. 5-40 cm, **d**. 10-20 cm, **e**. 10-40 cm, and **f**. 20-40 cm. Blue for k1, red for k2, and green for k3.

Fourth-order:

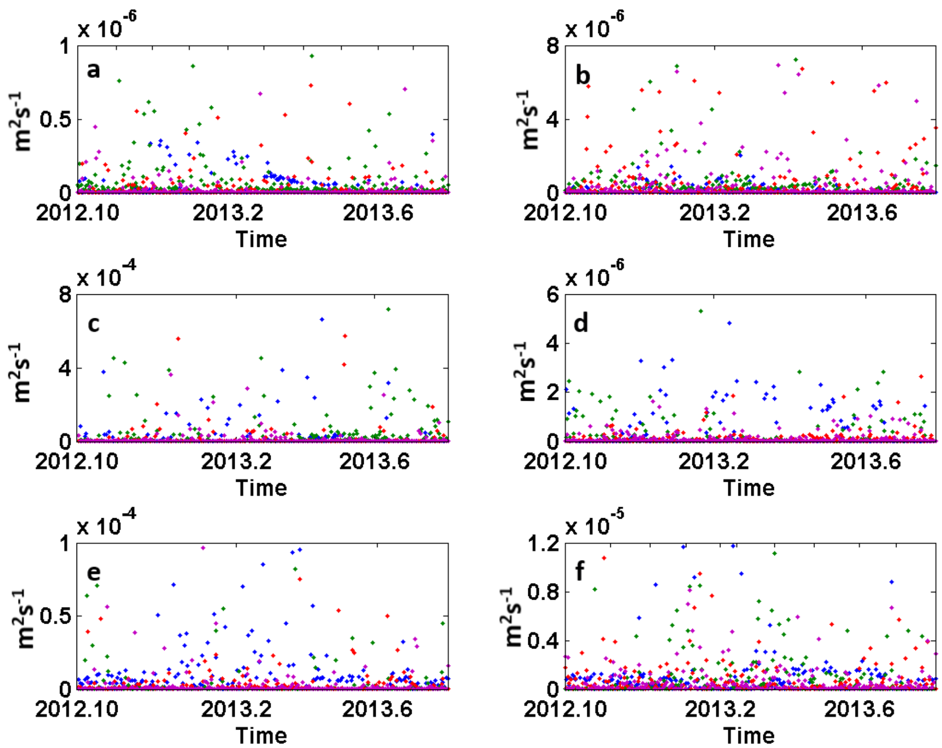

Figure 8. Soil thermal diffusivities of six different depths on the surface calculated by fourth-order Fourier series. **a**. 5-10 cm, **b**. 5-20 cm, **c**. 5-40 cm, **d**. 10-20 cm, **e**. 10-40 cm, and **f**. 20-40 cm. Blue for k1, red for k2, green for k3, and purple for k4

4.4 Bias analysis of fitting soil temperature under Fourier series

Soil temperature changes are complex and affected by many factors. Soil convective heat exchanges have a significant contribution to soil temperature oscillations. Therefore, using the Fourier series to accurately describe the diurnal variation in shallow soil can reduce the bias caused by assuming that the temperature of the soil surface follows a single sine wave (Wang et al., 2010). In this section, the soil temperature fitted by the 1st-, 2nd-, 3rd-, and 4th-order Fourier series is compared with the measured soil temperature. The goodness of fit of different regression models is usually determined using the coefficient of determination (R^2) (Wang et al., 2019). The coefficient of determination, also known as the determination coefficient, and the decision index represent the amount by which the independent variable explains the percentage change of the dependent variable. Therefore, the larger the coefficient of determination, the better the regression effect of the model. R^2 can be expressed as follows:

$$R^2 = 1 - \frac{\sum (y - \hat{y})^2}{\sum (y - \bar{y})^2}$$

In Figure 9, several sets of data at the same depth (a1, b1, c1, d1; a2, b2, c2, d2; a3, b3, c3, d3; a4, b4, c4, d4; a5, b5, c5, d5; a6, b6, c6, d6) are used for comparison. In the six sets of data, the R^2 value is ordered as follows fourth-order > third-order > second-order > first-order. In addition, the fourth-order Fourier series is used to fit the soil temperature to depths of 5 cm, 10 cm, and 20 cm, R^2 is above 0.96, and the highest is 0.9999. The minimum value of the fitting result with respect to the first-order Fourier series is less than 0.5, indicating that the fitting result also improves as the fitting order increases. At depths of 80 cm and 180 cm, the soil change was close to a linear change due to the layered soil (Figure 10); therefore, the results obtained by the Fourier series were weaker than that at other levels. Moreover, studies have shown that using the fifth-order Fourier series to simulate the daily variation in the soil temperature field is quite accurate (Liu et al., 1991). Too many harmonics will cause oscillations, which are not only difficult to calculate but also reduce the accuracy.

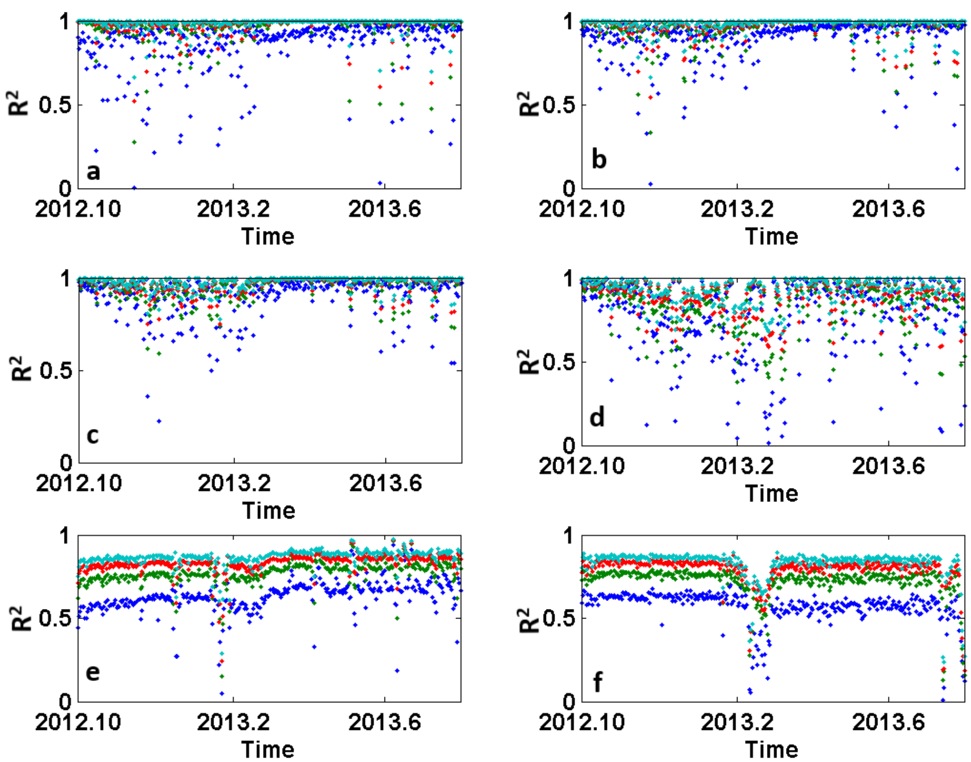

Figure 9. Bias for soil temperature fitted by Fourier series. Results at **a**. 5 cm; **b**. 10 cm; **c**. 20 cm; **d**. 40 cm; **e**. 80 cm; and **f**. 180 cm. Dark blue for the 1st order, green for the 2nd order, red for the 3rd order, and light blue for the fourth order.

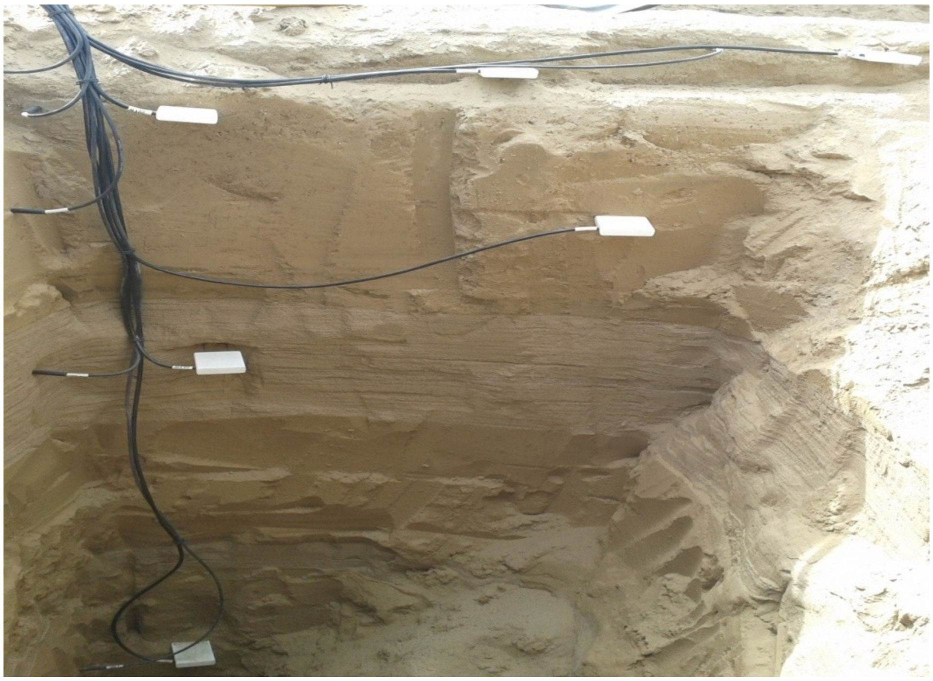

Figure 10. Soil layer structure.

5 Conclusions

In this paper, the results of soil thermal diffusivities obtained from different boundary conditions under the thermal conduction equation are compared horizontally. A new model for solving the thermal diffusivity of the thermal conduction-convection equation under the Fourier boundary condition is proposed, and the results of soil temperature simulations with different order Fourier series are compared. The results show that (1) the amplitude method and phase method are based on a single temperature sine wave, which is used to describe the general soil; however, the accuracy is not high enough and the disadvantages are especially obvious when encountering multiple temperature extreme values. The logarithmic method and the arctangent method are performed four times a day, which can partially reflect the nonperiodic change of soil temperature; however, the data utilization rate is not high enough and the accuracy of the obtained results is also low. The Laplace method does not have a clear soil temperature boundary function and thus can better address extreme weather effects or nonperiodic changes in soil temperature. (2) When solving the thermal conduction equation by a numerical method, format 2 (Crank-Nichalson-Sch format) is unconditionally stable and the data utilization rate is higher. The obtained soil thermal diffusivity is less discrete, and the result is more accurate. (3) When the thermal conduction-convection equation is used to solve the soil thermal diffusivity under the Fourier series boundary condition, the n-order soil thermal diffusivity k_n represents the influence of different fluctuations of soil temperature on the total soil thermal diffusivity and its contribution; when the soil temperature is simulated by the Fourier series, the result becomes more accurate as the order n becomes larger than the measured soil temperature. In addition, the Fourier series performs well in simulating and solving soil thermal properties. The model for solving the soil thermal diffusivity by the thermal conduction-convection equation under the Fourier boundary condition proposed in this paper has certain significance in solving the problem of thermal diffusivity calculation. However, it assumes that soil temperature changes have a certain periodicity, which may cause some problems when addressing nonperiodic changes in soil. According to the previous test, the Laplace method of the thermal conduction equation performs well in response to nonperiodic changes in soil temperature. However, the Laplace transform process is more difficult and the solution is more complicated. Therefore, this method should be applied to the thermal conduction-convection equation in a more convenient and feasible way, and it is expected to further contribute to the solution of soil thermal diffusivity.

Soil is an extremely important component of the biogeochemical cycles. The thermal properties of soil affect the survival and functioning conditions of vegetation, soil microorganisms, and soil enzymes. This work starts with the improvement of soil thermal diffusivity, which is one of the thermal properties of soil and is helpful for further understanding soil thermal properties and soil thermal activities. Thus, this work is significant for understanding biogeochemical cycles.

Acknowledgments

Financial support from the National Key R&D Program of China (2018YFB1502800), the National Natural Science Foundation of China (Grant No. 41875017) and the Opening Fund of Key Laboratory of Desert and Desertification, CAS (No. KLDD-2020-004) is gratefully acknowledged. The authors declare no competing financial interest. The authors would also like to thank the anonymous reviewers for their constructive comments and suggestions that significantly improved the quality of our manuscript.

Data availability statement

Datasets for this research are included in this paper (and its supplementary information files): Yang, L., Gao, X., Lv, F., Hui, X., Ma, L., & Hou, X. (2017). Study on the local climatic effects of large photovoltaic solar farms in desert areas. Solar Energy, 144, 244–253. https://doi.org/10.1016/j.solener.2017.01.015

References

Abramoff, R. Z., & Finzi, A. C. (2015). Are above- and below-ground phenology in sync? *New Phytologist, 205*(3), 1054–1061. https://doi.org/10.1111/nph.13111

Ahmed, N., & Rao, K. R. (1975). *Orthogonal transforms for digital signal processing*. Berlin, Heidelberg: Springer Science & Business Media.

Bhumralkar, C. M. (1975). Numerical experiments on the computation of ground surface temperature in an atmospheric general circulation model. *Journal of Applied Meteorology, 14*(7), 1246–1258. https://doi.org/10.1175/1520-0450(1975)014<1246:neotco>2.0.co;2

Carslaw, H. S., & Jaeger, J. C. (1959). *Conduction heat in solids*. Oxford, UK: Oxford Science Publications.

Dai, C. Y., Gao, Z. Q., Wang, L. L., & Fan, J. H. (2009). Intercomparison between two soil temperature algorithms. *Chinese Journal of Atmospheric Sciences, 33*(1), 135–144.

de Silans, A. M. B. P., Monteny, B. A., & Lhomme, J. P. (1996). Apparent soil thermal diffusivity, a case study: HAPEX-Sahel experiment. *Agricultural and Forest Meteorology, 81*(3-4), 201–216. https://doi.org/10.1016/0168-1923(95)02323-2

Duan, H. D., Zhang, X. Z., Ma, L., Li, Z. L., Zhang, Z., Zhang, Z. G., et al. (2016). Fourier series sidereal filtering in GPS dynamic deformation analysis. *Journal of Geodesy and Geodynamics, 36*(7), 610–616.

Fang, Y. L., Sun, S. F., Li, Q., & Chen, W. (2010). The optimization of parameters of land surface model in arid region and the simulation of land-atmosphere interaction. *Chinese Journal of Atmospheric Sciences, 34*(2), 290–306.

Gao, X. Q., Yang, L. W., Lyu, F., Ma, L. Y., & Li, H. L. (2016). Observational study on the impact of the large solar farm on air temperature and humidity in desert areas of Golmud. *Acta Energiae Solaris Sinica, 37*(11), 2909–2915.

Gao, Z. (2005). Determination of soil heat flux in a tibetan short-grass prairie. *Boundary-Layer Meteorology, 114*(1), 165–178. https://doi.org/10.1007/s10546-004-8661-5

Gao, Z., Fan, X., & Bian, L. (2003). An analytical solution to one-dimensional thermal conduction-convection in soil. *Soil Science, 168*(2), 99–107. https://doi.org/10.1097/00010694-200302000-00004

Goto, S., Yamano, M., & Kinoshita, M. (2005). Thermal response of sediment with vertical fluid flow to periodic temperature variation at the surface. *Journal of Geophysical Research, 110*(B1), B01106. https://doi.org/10.1029/2004jb003419

Hillel, D. (2014). *Introduction to environmental soil physics*. San Diego, CA: Elsevier Academic Press.

Horton, R., Wierenga, P. J., & Nielsen, D. R. (1983). Evaluation of methods for determining the apparent thermal diffusivity of soil near the surface. *Soil Science Society of America Journal, 47*(1), 25–32. https://doi.org/10.2136/sssaj1983.03615995004700010005x

Hu, G., Zhao, L., Wu, X., Li, R., Wu, T., Xie, C., et al. (2015). New Fourier-series-based analytical solution to the conduction–convection equation to calculate soil temperature, determine soil thermal properties, or estimate water flux. *International Journal of Heat and Mass Transfer, 95*, 815–823. https://doi.org/10.1016/j.ijheatmasstransfer.2015.11.078

Kane, D. L., Hinkel, K. M., Goering, D. J., Hinzman, L. D., & Outcalt, S. I. (2001). Non-conductive heat transfer associated with frozen soils. *Global and Planetary Change, 29*(3-4), 275–292. https://doi.org/10.1016/s0921-8181(01)00095-9

Lee, S. H., Kim, M. S., Kim, J. G., & Kim, S. O. (2020). Use of soil enzymes as indicators for contaminated soil monitoring and sustainable management. *Sustainability, 12*(19), 8209. https://doi.org/10.3390/su12198209

Li, N., Jia, L., & Lu, J. (2015). An improved algorithm to estimate the surface soil heat flux over a heterogeneous surface: A case study in the Heihe river basin. *Science China Earth Sciences, 58*(7), 1169–1181. https://doi.org/10.1007/s11430-014-5041-y

Liang, H. Q. (1982). Introducing into Fourier series a concept of coordinate set for analyzing signals in digital filters. *Automation of Electric Power Systems, 3*, 13–24.

Liu, Q. Q., Wei, D. P., Sun, Z. T., & Han, P. (2014). Review of related researches on calculation of shallow ground heat transfer. *Progress in Geophysics, 29*(6), 2510–2517.

Liu, S. H., Cui, Y., & Liu, H. P. (1991). Determination of thermal diffusivity of soil and its application. *Quarterly Journal of Applied Meteorology, 2*(4), 338–345.

Liu, Y., He, Q., Zhang, H., & Mamtimin, A. (2012). Improving the CoLM in Taklimakan Desert hinterland with accurate key parameters and an appropriate parameterization scheme. *Advances in Atmospheric Sciences, 29*(2), 381–390. https://doi.org/10.1007/s00376-011-1068-6

Luo, Y., Sherry, R., Zhou, X., & Wan, S. (2009). Terrestrial carbon-cycle feedback to climate warming: Experimental evidence on plant regulation and impacts of biofuel feedstock harvest. *GCB Bioenergy, 1*(1), 62–74. https://doi.org/10.1111/j.1757-1707.2008.01005.x

Munir, T. M., Perkins, M., Kaing, E., & Strack, M. (2015). Carbon dioxide flux and net primary production of a boreal treed bog: Responses to warming and water-table-lowering simulations of climate change. *Biogeosciences, 12*(4), 1091–1111. https://doi.org/10.5194/bg-12-1091-2015

Oelke, C., & Zhang, T. (2004). A model study of circum-Arctic soil temperatures. *Permafrost and Periglacial Processes, 15*(2), 103–121. https://doi.org/10.1002/ppp.485

Paul, K. I., Polglase, P. J., Smethurst, P. J., O'Connell, A. M., Carlyle, C. J., & Khanna, P. K. (2004). Soil temperature under forests: a simple model for predicting soil temperature under a range of forest types. *Agricultural and Forest Meteorology, 121*(3-4), 167–182. https://doi.org/10.1016/j.agrformet.2003.08.030

Rustad, L., Campbell, J., Marion, G., Norby, R., Mitchell, M., Hartley, A., et al. (2001). A meta-analysis of the response of soil respiration, net nitrogen mineralization, and aboveground plant growth to experimental ecosystem warming. *Oecologia, 126*(4), 543–562. https://doi.org/10.1007/s004420000544

Shao, M., Horton, R., & Jaynes, D. B. (1998). Analytical solution for one-dimensional heat conduction-convection equation. *Soil Science Society of America Journal, 62*(1), 123–128. https://doi.org/10.2136/sssaj1998.03615995006200010016x

Usowicz, B. (1996). Spatial variability of soil thermal properties in cultivated fields. *Soil and Tillage Research, 39*(1-2), 85–100. https://doi.org/10.1016/s0167-1987(96)01038-0

Van Wijk, W. R., & de Vries, D. A. (1963). Periodic temperature variations in a homogeneous soil. In W. R. Van Wijk (Ed.), *Physics of plant environment* (pp. 103–143). Amsterdam: North-Holland Publishing Company.

Wang, G., Zhou, Y., Xu, X., Ruan, H., & Wang, J. (2013). Temperature sensitivity of soil organic carbon mineralization along an elevation gradient in the Wuyi mountains, China. *PLoS One, 8*(1), e53914. https://doi.org/10.1371/journal.pone.0053914

Wang, L., Gao, Z., & Horton, R. (2010). Comparison of six algorithms to determine the soil apparent thermal diffusivity at a site in the Loess Plateau of China. *Soil Science, 175*(2), 51–60. https://doi.org/10.1097/ss.0b013e3181cdda3f

Wang, X. P., Lin, J. X., Wu, J. W., & Gao, M. J. (2019). Adaptive association rule mining algorithm based on determination coefficient. *CAAI Transactions on Intelligent Systems*. https://doi.org/10.11992/tis.201809030

Xu, X., Sherry, R. A., Niu, S., Li, D., & Luo, Y. (2013). Net primary productivity and rain-use efficiency as affected by warming, altered precipitation, and clipping in a mixed-grass prairie. *Global Change Biology, 19*(9), 2753–2764. https://doi.org/10.1111/gcb.12248

Yang, L., Gao, X., Lv, F., Hui, X., Ma, L., & Hou, X. (2017). Study on the local climatic effects of large photovoltaic solar farms in desert areas. *Solar Energy, 144*, 244–253. https://doi.org/10.1016/j.solener.2017.01.015

Yue, P., Zhang, Q., Yang, J. H., Li, H. L., Sun, X. Y., & Yang, Q. G. (2011). Surface heat flux and energy budget for semi- arid grassland on the Loess Plateau. *Acta Ecologica Sinica, 31*(22), 6866–6876. https://doi.org/10.7498/aps.62.209201

Zhang, H. H., Liu, S. H., Wei, Z. G., Lu, S. H., Hou, X. H., Wen, J., et al. (2011). Comparative study of computing methods of soil temperature on different underlying surfaces. *Acta Scientiarum Naturalium Universitatis Pekinensis, 47*(6), 1025–1033.

Zhang, X., Gao, Z., & Wei, D. (2012). The sensitivity of ground surface temperature prediction to soil thermal properties using the simple biosphere model (SiB2). *Advances in Atmospheric Sciences, 29*(3), 623–634. https://doi.org/10.1007/s00376-011-1162-9

Zheng, H., & Liu, S. H. (2013). Land surface parameterization and modeling over desert. *Chinese Journal of Geophysics, 56*(7), 2207–2217.